



Original Article



m1A Epitranscriptomic Control of NUPR1 by YTHDF1 Exacerbates Metabolic Dysregulation in Nonalcoholic Fatty Liver Disease

Nan Luo^{1#}, Zhihai Xu^{2#}, Dongmei Zhao³, Xue Yang², Yu Tian^{2*} and Rongkuan Li^{1*}

¹Department of Infection, The Second Hospital of Dalian Medical University, Dalian, Liaoning, China; ²Department of Vascular Surgery, The Second Hospital of Dalian Medical University, Dalian, Liaoning, China; ³Shanghai Fifth People's Hospital, Fudan University, Shanghai, China

Received: November 01, 2025 | Revised: January 06, 2026 | Accepted: March 03, 2026 | Published online: April 02, 2026

Abstract

Background and Aims: Nonalcoholic fatty liver disease (NAFLD) is a prevalent metabolic disorder with a complex pathogenesis. Although epitranscriptomic modifications such as N6-methyladenosine (m6A) have been implicated in NAFLD, the role of N1-methyladenosine (m1A) and its regulators is largely unexplored. Recently, YTHDF1, a well-characterized m6A reader, was also shown to recognize m1A; however, the functional consequences of this dual specificity are unknown. This study aimed to investigate the role of YTHDF1 in NAFLD pathogenesis and to explore whether its function is mediated through recognition of RNA methylation modification on specific target mRNAs. **Methods:** Expression of YTHDF1 in NAFLD was analyzed in the GEO database. Loss-of-function studies for YTHDF1 were conducted *in vivo* (high-fat diet-fed mice) and *in vitro* (free fatty acid-treated HepG2 cells) in models of NAFLD. We employed RNA-seq and m1A-MeRIP-seq to identify key targets, followed by mechanistic validation of the YTHDF1–m1A–NUPR1 axis using biochemical, histological, and mRNA stability assays. **Results:** We identified a critical role for YTHDF1 in promoting hepatic steatosis. NUPR1, a stress-induced transcriptional regulator, undergoes m1A modification. YTHDF1 directly binds to m1A-modified NUPR1 mRNA, enhancing its stability, thereby leading to elevated NUPR1 protein levels. Functionally, upregulated NUPR1 acts as a core driver of NAFLD pathogenesis by activating lipogenic and suppressing fatty acid β -oxidation genes, thereby exacerbating hepatic lipid accumulation. **Conclusions:** Our study unveils a novel epitranscriptomic mechanism in which YTHDF1, functioning as a dual-specificity reader, governs NAFLD progression through the m1A–NUPR1 axis. This not only expands the understanding of RNA modification recognition but also establishes the

YTHDF1–m1A–NUPR1 pathway as a promising therapeutic target for metabolic liver disease.

Citation of this article: Luo N, Xu Z, Zhao D, Yang X, Tian Y, Li R. m1A Epitranscriptomic Control of NUPR1 by YTHDF1 Exacerbates Metabolic Dysregulation in Nonalcoholic Fatty Liver Disease. J Clin Transl Hepatol 2026. doi: 10.14218/JCTH.2025.00570.

Introduction

Nonalcoholic fatty liver disease (NAFLD) is a spectrum of liver disorders that originate with simple steatosis (SS) and may advance to nonalcoholic steatohepatitis (NASH). This pathological continuum is defined by the initial accumulation of lipids in hepatocytes, which may progressively evolve into more severe liver damage, including fibrosis, cirrhosis, and hepatocellular carcinoma.¹ With a prevalence of nearly 25% globally, NAFLD has become a pressing worldwide health issue. Its incidence is projected to continue its upward trend in the foreseeable future.² Emerging as a metabolic disorder with multisystem implications, NAFLD demonstrates profound pathophysiological connections with insulin resistance, obesity, type 2 diabetes, and cardiovascular complications.^{3,4} Owing to its compelling metabolic associations, it is increasingly referred to as metabolic dysfunction-associated fatty liver disease.⁵

The progression of NAFLD is known to be significantly influenced by epitranscriptomic regulation. Key among these regulatory mechanisms are reversible RNA methylation marks, particularly N6-methyladenosine (m6A) and N1-methyladenosine (m1A), which post-transcriptionally control gene expression by modulating mRNA stability, splicing, and translational efficiency. Functioning as a principal “reader” of the m6A modification, YTHDF1 binds to methylated transcripts and enhances their translation. A growing amount of research has implicated this m6A-sensing capability of YTHDF1 as a key driver in the pathogenesis of NAFLD.^{6–8} It promotes hepatic steatosis by enhancing the translation efficiency of key lipogenic genes and may exacerbate inflammation and fibrosis by upregulating pro-inflammatory mediators like TNF- α and IL-6.^{9,10} Crucially, evidence shows

Keywords: Non-alcoholic fatty liver disease; YTHDF1 protein; RNA methylation; NUPR1 protein; Lipid metabolism; RNA stability.

[#]Contributed equally to this work.

***Correspondence to:** Rongkuan Li, Department of Infection, The Second Hospital of Dalian Medical University, Dalian, Liaoning 116023, China. ORCID: <https://orcid.org/0000-0002-2927-7017>. E-mail: dalianlrk@126.com; Yu Tian, Department of Vascular Surgery, The Second Hospital of Dalian Medical University, Dalian, Liaoning 116023, China. ORCID: <https://orcid.org/0000-0001-6378-1199>. E-mail: dlvascuty@126.com.

that YTHDF1 knockdown ameliorates NAFLD phenotypes in mice, suggesting substantial therapeutic potential, though human data remain scarce.⁷ Furthermore, the functional scope of YTHDF1 has recently expanded. Beyond its canonical role in m6A recognition, compelling studies now indicate that YTHDF1 also acts as a reader for m1A modifications. This discovery positions YTHDF1 at the nexus of two major epitranscriptomic pathways, significantly broadening its potential regulatory influence on gene expression. However, while its m6A-related pro-NAFLD mechanisms are becoming clearer, the specific biological consequences of its m1A recognition capability remain entirely unexplored in the context of hepatic lipid metabolism and NAFLD.

Mechanistically, we identified that the mRNA of NUPR1, a stress-induced transcriptional regulator, undergoes m1A modification, which is specifically recognized by YTHDF1. This recognition enhances NUPR1 mRNA stability and translation, thereby elevating NUPR1 protein levels. Consequently, NUPR1 acts as a core driver in NAFLD by activating lipogenic transcriptional programs and suppressing fatty acid oxidation, ultimately exacerbating hepatic lipid accumulation and inflammation. The amelioration of steatosis upon disruption of either YTHDF1 or NUPR1 underscores the YTHDF1–m1A–NUPR1 axis as a promising therapeutic target.

Our findings reveal a novel regulatory mechanism wherein YTHDF1, traditionally known as an m6A reader, also functions as an m1A reader to govern NUPR1 expression in NAFLD. This expands the understanding of YTHDF1's dual specificity in RNA modification recognition and highlights m1A-mediated epitranscriptomic regulation as a critical contributor to metabolic liver disease.

Methods

Animal experiments

For the establishment of a NAFLD mouse model, 6-week-old C57BL/6J mice were first acclimatized on a normal diet (ND, D102102C) for one week. To induce hepatic steatosis, the mice were subsequently fed a high-fat diet (HFD, 12109C) from weeks 8 to 16, with ND as the control. To achieve hepatic YTHDF1 knockdown, 16-week-old mice received a tail vein injection of an adeno-associated virus carrying shYTHDF1 (Genepharma, rAAV8-TBG-shYTHDF1), and a corresponding control virus (Genepharma, rAAV-TBG-Ctrl) was used as control. Two weeks after injection, the mice were euthanized, and relevant tissues and blood were harvested for subsequent analysis. The study protocol received approval from the Laboratory Animal Center, Dalian Medical University (AEE23139).

Oil Red O staining

Liver tissue cryosections or cells were fixed with formaldehyde solution and soaked in 60% isopropanol after washing with distilled water, then stained with Oil Red O working solution (Meilunbio). After washes with distilled water, nuclear counterstaining was performed using hematoxylin staining solution.¹¹ After washing and dehydration, images were acquired with an Olympus light microscope.

Cell culture and transfection

HepG2 cells, sourced from the American Type Culture Collection, were maintained under standard conditions in DMEM (Meilunbio) supplemented with 10% fetal bovine serum (Gibco). An *in vitro* model of hepatic steatosis was established by subjecting cells to 12 h serum starvation, followed by 24 h treatment with 0.5 mM free fatty acids (FFA). The FFA was composed of sodium oleate (Sigma) and sodium palmitate

(Sigma) at a 2:1 ratio.

Short hairpin RNAs (shRNAs) targeting YTHDF1 and a plasmid overexpressing NUPR1 were commercially synthesized by GenePharma. Transfections were performed using Lipofectamine 3000 (Invitrogen) following the manufacturer's protocol.¹²

Western blot

Western blot analysis was performed according to a previously described protocol.¹³ Briefly, cells were lysed using RIPA buffer (Beyotime) supplemented with protease and phosphatase inhibitors (Roche). Protein concentration was determined with the BCA Protein Assay Kit (Thermo Fisher Scientific). Samples containing 20 µg of protein were separated by SDS-PAGE (Bio-Rad) and transferred to PVDF membranes (Millipore). The membranes were blocked with 5% non-fat milk in TBST and then incubated with primary antibodies, followed by HRP-conjugated secondary antibodies (Thermo Fisher Scientific) for 1 h at room temperature. Protein bands were visualized using an ECL detection kit (Bio-Rad). The following primary antibodies were used: anti-SCD1 (Proteintech, 28678-1-AP), anti-FADS1 (Proteintech, 10627-1-AP), anti-FABP1 (Proteintech, 13626-1-AP), anti-CPT1A (Proteintech, 66039-1-Ig), anti-YTHDF1 (Proteintech, 17479-1-AP), anti-NUPR1 (Proteintech, 15056-1-AP), and anti-GAPDH (Proteintech, 60004-1-Ig).

PCR assay

Total RNA was isolated using RNA-Easy Isolation Reagent (Vazyme) according to the manufacturer's instructions. RNA quality was analyzed by a NanoDrop 2000c spectrophotometer. Complementary DNA was synthesized using HiScript II Q RT SuperMix for qPCR (Vazyme). Real-time reverse transcription PCR was performed using ChamQ Universal SYBR qPCR Master Mix in a qTOWER Real-time PCR Thermal Cycler (Analytik Jena). Relative gene expression was normalized to β-actin using the standard 2^{-ΔΔCt} quantification method.¹⁴ The primer sequences are listed in Supplementary Table 1.

Hematoxylin and eosin (H&E) staining and Immunohistochemistry (IHC)

Formalin-fixed, paraffin-embedded tissues were sectioned at 5 µm thickness. H&E and IHC detection were performed using standard protocols.¹¹ The primary antibodies used for IHC were anti-YTHDF1 (Proteintech, 17479-1-AP), anti-NUPR1 (Proteintech, 15056-1-AP), anti-SCD1 (Proteintech, 28678-1-AP), anti-FADS1 (Proteintech, 10627-1-AP), anti-FABP1 (Proteintech, 13626-1-AP), and anti-CPT1A (Proteintech, 66039-1-Ig). Histopathological assessment was conducted by pathologists. Protein expression was semi-quantitatively assessed using the H-score method.¹⁵

mRNA stability

After seeding in 6-well plates and culturing overnight, HepG2 cells were exposed to 5 µg/mL actinomycin D (act-D, MedChem Express, HY-17559) to block RNA transcription. Cells were then harvested at 0, 2, 4, and 6 h for subsequent quantification of mRNA levels at each time point.

Biochemical analysis

Serum alanine aminotransferase (ALT) and aspartate aminotransferase (AST) levels were measured using an automatic biochemistry analyzer. Mouse serum triglycerides were collected and analyzed using commercial kits (Nanjing Jincheng Bioengineering Institute, C009-2-1 and C010-2-1) according to the manufacturer's instructions.

RNA immunoprecipitation (RIP)

To investigate RNA-YTHDF1 interactions, RIP was performed using the Magna RIP™ RNA-Binding Protein Immunoprecipitation Kit (Millipore).¹⁶ Briefly, cells were lysed in RIP lysis buffer. The cell lysates were then incubated with magnetic beads conjugated with either an anti-YTHDF1 antibody or a control IgG. After a series of washes, RNA was isolated from the immunoprecipitated complexes using TRIzol reagent (Invitrogen).

MeRIP-seq

Following the manufacturer's instructions for the MeRIP Kit (BersinBio), RNA samples extracted from cells were fragmented into segments of approximately 200 nt. Protein A/G magnetic beads were incubated with m1A antibody under rotation at room temperature for 1 h to allow antibody-bead conjugation. The RNA fragments were then incubated with the antibody-bound beads under rotation at 4 °C for 4 h to facilitate RNA-antibody binding. After incubation, the complex was washed, and the bound RNA was subsequently eluted.^{17,18} The alkaline-treated IP and input samples were then used to construct RNA sequencing libraries using the GenSeq® Low Input Whole RNA Library Prep Kit (GenSeq). The quality of the prepared libraries was assessed using an Agilent 2100 Bioanalyzer (Agilent), followed by high-throughput sequencing on a NovaSeq platform (Illumina).

Data analysis

The experimental data were analyzed and plotted using Excel and GraphPad 22.0 software. All data were represented as mean ± standard error of the mean of at least three independent experiments. Statistical significance was assessed by an unpaired Student's t-test unless otherwise indicated. *P*-values < 0.05 were considered statistically significant.

Results

Abnormal expression of YTHDF1 is found in NAFLD

Although m6A-related genes have been demonstrated to play critical roles in the progression of NAFLD, a comprehensive analysis of the differential expression of all m6A regulatory genes across normal liver tissue, hepatic steatosis, and NAFLD remains lacking. We initially focused on the dysregulated m6A-related genes through the analysis of NAFLD-related GEO datasets GSE48452 and GSE89632. As shown in Figure 1A and B, YTHDC1/2 was lower in NASH than in HC. WTAP, ALKBH1, RBM15, HNRNPC, and HNRNPA2B1 expression was lower in SS and NASH than in HC. Others, such as METTL3/14, RBM15B, ZC3H13, KIAA1429, CBLL1, ALKBH5, FTO, YTHDF2/3, IGF2BP1, FMR1, LRPPRC, and ELVAL1, did not show significant differences among the groups. However, expression of YTHDF1 in SS and NASH was higher in NASH than in SS, with the highest expression observed in NASH among the three groups.

To elucidate the potential role of YTHDF1 in NAFLD pathogenesis, we used a well-established diet-induced mouse model. After maintaining the animals on either an HFD or an ND as a control for four months, HFD-fed mice showed a remarkable gain in both body and liver mass (Fig. 2A and B). Subsequent biochemical analysis confirmed elevations in serum ALT, AST, and triglyceride levels in this group (Fig. 2C–E). Histologically, H&E staining revealed diffuse macrovesicular steatosis in hepatocytes of HFD-fed mice, which was not observed in the ND group (Fig. 2F). Consistent with this, Oil Red O staining showed markedly more pronounced lipid

deposition in the HFD group compared to the ND group (Fig. 2G). Having confirmed the successful induction of NAFLD, we then assessed the hepatic levels of YTHDF1.

A significant upregulation of YTHDF1 was observed in the livers of HFD-fed mice compared to controls (Fig. 2H). As lipid accumulation is a pivotal event in NAFLD, we established an *in vitro* model by treating HepG2 cells with FFA for 24 h. This treatment successfully induced lipid droplet accumulation, as evidenced by Oil Red O staining (Fig. 2I). Consistent with the *in vivo* findings, YTHDF1 expression was also markedly elevated in FFA-treated cells (Fig. 2J). These results strongly suggest an association between YTHDF1 and NAFLD.

YTHDF1 suppression decreases lipidosis in liver cells

To investigate whether the increased YTHDF1 expression contributes to the development of hepatic steatosis, we established a YTHDF1 knockdown cellular model (Fig. 3A) and assessed intracellular lipid levels using Oil Red O staining. The results demonstrated that silencing YTHDF1 significantly reduced lipid droplet accumulation in hepatocytes (Fig. 3B). We also established a hepatic YTHDF1-knockdown mouse model by tail vein injection of an adenovirus expressing YTHDF1-specific shRNA. Two weeks after injection, mice with YTHDF1 suppression displayed decreased body and liver weight as well as reduced ALT and AST levels (Supplementary Fig. 1A–D). Oil Red O staining confirmed that the livers of these mice had decreased lipid accumulation (Fig. 3C). Given that SREBP1 controls the transcription of lipogenic genes such as FADS1, FABP1, and SCD1, and that CPT1A's impaired activity directly shunts fatty acids away from mitochondrial β -oxidation, promoting lipid droplet accumulation, we tested the expression of SREBP1, FADS1, FABP1, SCD1, and CPT1A both *in vivo* and *in vitro*. We found that SREBP1, FADS1, FABP1, and SCD1 levels were significantly decreased in cells treated with FFAs (Fig. 3D) and in the livers of HFD-fed mice after shYTHDF1 knockdown (Fig. 3E and F), compared to cells without YTHDF1 knockdown or control mice under the same feeding condition. In contrast, the expression level of CPT1A exhibited an opposite trend to that of these proteins (Fig. 3D and F). These data suggest that silencing YTHDF1 may inhibit hepatic lipogenesis both *in vivo* and *in vitro*.

NUPR1 may be regulated by YTHDF1 through reorganization of its m1A modification

RNA-seq analysis between FFA-treated and untreated HepG2 cells revealed 442 differentially expressed genes. Among these, 354 genes were upregulated and 88 were downregulated in the FFA-treated group relative to controls (Fig. 4A and B). By performing m1A analysis via MeRIP-seq in HepG2 cells, we identified 6,490 peaks and 3,901 significantly enriched transcripts. To decipher the sequence preference of m1A methylation, we conducted motif analysis on all reliable peaks from our m1A-MeRIP-seq data. As shown in Figure 4C, the sequence logo showed the top three m1A motifs enriched in HepG2 cells treated with FFA. We mapped the m1A peaks to different functional regions of mRNAs to investigate their potential regulatory roles. As shown in Figure 4D, the m1A modifications exhibited a distinctive distribution pattern. The m1A peaks were predominantly enriched in the 5' and 3' untranslated regions (UTRs), with relative depletion in the coding sequence and around the start codon. This specific localization pattern implies that m1A may regulate mRNA translation efficiency and stability. We ranked the genes involved in m1A-MeRIP-seq against differentially expressed genes after FFA treatment (Fig. 4E) and selected 10 candidate genes with putative roles in NAFLD for further

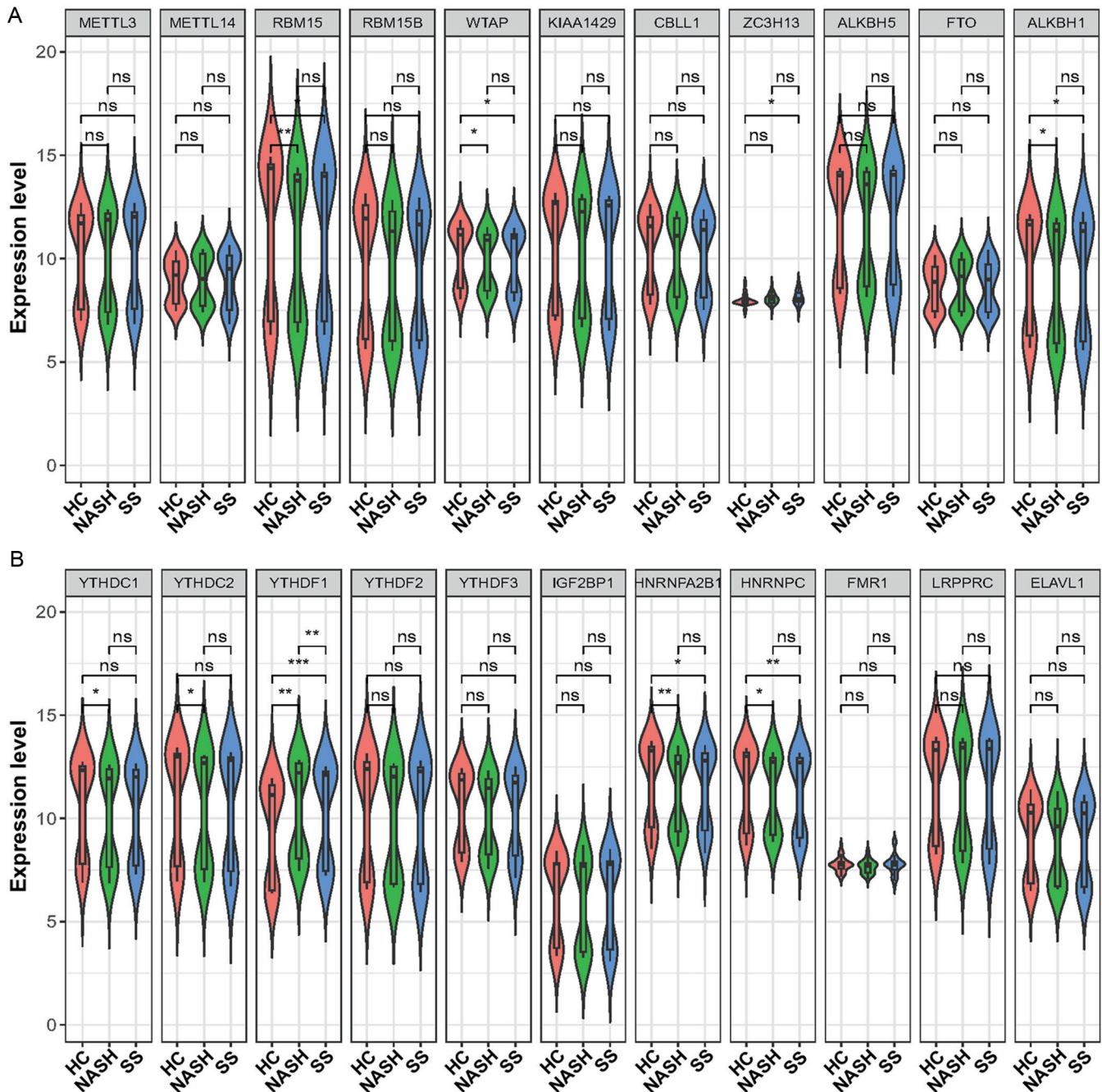


Fig. 1. Expression of m6A regulators in NAFLD based on GEO database analysis. Analysis of GEO datasets (GSE48452 and GSE89632) identified differential expression profiles of m6A regulatory genes in human liver tissues from HC, SS, and NASH. (A) Expression analysis of METTL3, METTL14, RBM15, RBM15B, WTAP, KIAA1429, CBLL1, ZC3H13, ALKBH5, FTO and ALKBH1. (B) Expression analysis of YTHDC1, YTHDC2, YTHDF1, YTHDF2, YTHDF3, IGF2BP1, HNRNPA2B1, HNRNPC, FMR1, LRPPRC and ELAVL1. * $P < 0.05$, ** $P < 0.01$, *** $P < 0.001$; ns, not significant; GEO, Gene Expression Omnibus; NAFLD, Non-alcoholic fatty liver disease; HC, healthy controls; SS, simple steatosis; NASH, nonalcoholic steatohepatitis.

verification by RT-qPCR. Among the 10 candidate targets of YTHDF1, only NUPR1 expression was higher in FFA-treated cells than in untreated cells and decreased after YTHDF1 knockdown (Fig. 4F and Supplementary Fig. 2A–I). Furthermore, in contrast to the potential m1A modification sites found in NUPR1, our analysis using the Whistle web server (<http://180.208.58.19/whistle/index.html>) predicted the absence of m6A sites. We subsequently validated the m1A

modification on NUPR1 mRNA via m1A-RIP-PCR (Fig. 4G). To further confirm the direct interaction between YTHDF1 protein and NUPR1 mRNA, we performed RNA RIP using an antibody specific to YTHDF1, followed by PCR analysis of the bound RNA. The results demonstrated significant enrichment of NUPR1 mRNA in the YTHDF1 immunoprecipitate compared to the control IgG group (Fig. 4H). To determine if YTHDF1 regulates NUPR1 expression post-transcriptionally,

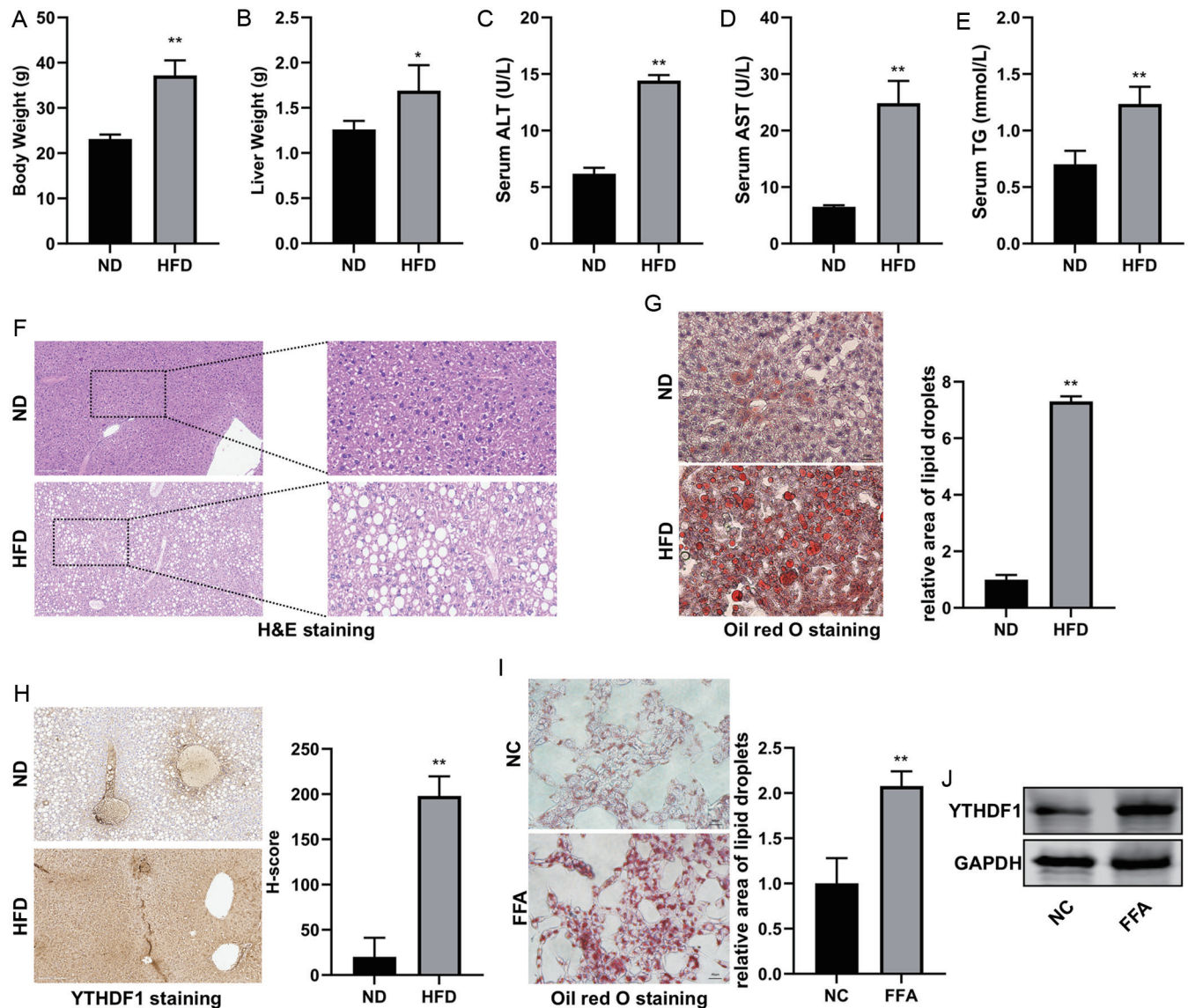


Fig. 2. Validation of YTHDF1 Expression in Experimental NAFLD Models. (A) Body weight and (B) liver weight of mice fed a ND or a HFD ($n = 5$). (C-E) Serum levels of ALT, AST, and TG in ND- and HFD-fed mice ($n = 5$). (F) Representative H&E stained liver sections from ND- and HFD-fed mice ($n = 5$). (G) Representative Oil Red O-stained liver sections and quantitative analysis from ND- and HFD-fed mice ($n = 5$). (H) Representative IHC staining and quantitative analysis of YTHDF1 in liver tissues from ND- and HFD-fed mice ($n = 5$). (I) Representative Oil Red O staining and quantitative analysis of FFA-treated and NC HepG2 cells. (J) Western blot analysis of YTHDF1 expression in FFA-treated and NC HepG2 cells. Data are shown as means \pm S.D. ** $P < 0.01$. NAFLD, Non-alcoholic fatty liver disease; ND, normal diet; HFD, high-fat diet; ALT, alanine aminotransferase; AST, aspartate aminotransferase; TG, triglycerides; H&E, hematoxylin and eosin; FFA, free fatty acids; NC, negative control.

we measured NUPR1 mRNA stability. Consistent with this notion, depleting YTHDF1 led to destabilization of NUPR1 mRNA in HepG2 cells (Fig. 4I). We then detected NUPR1 protein expression upon YTHDF1 knockdown and found that it was significantly reduced in HepG2 cells following FFA treatment (Fig. 4J). Collectively, these results indicate that NUPR1 is an m1A-modified gene whose expression is potentially regulated by YTHDF1, influencing its mRNA stability and translation.

Hepatic YTHDF1 controls lipogenesis by targeting NUPR1 mRNA

We tested the hypothesis that NUPR1 serves as a central mediator of YTHDF1-driven lipogenesis by determining if its overexpression would counteract the effects of YTHDF1 sup-

pression. We overexpressed NUPR1 in YTHDF1-knockdown HepG2 cells (Fig. 5A). As expected, NUPR1 overexpression greatly attenuated the effect of shYTHDF1 on the expression of key lipogenic genes (SREBP1, FADS1, FABP1, SCD1) and the fatty acid oxidation rate-limiting enzyme CPT1A (Fig. 5B and C). Notably, NUPR1 overexpression attenuated the inhibitory effect of shYTHDF1 on lipid droplet accumulation (Fig. 5D). These findings position NUPR1 as a key effector downstream of YTHDF1 in promoting hepatic lipid deposition.

Discussion

Hepatocyte lipotoxicity, driven by the imbalance between lipid acquisition and disposal, is a central pathogenic mechanism

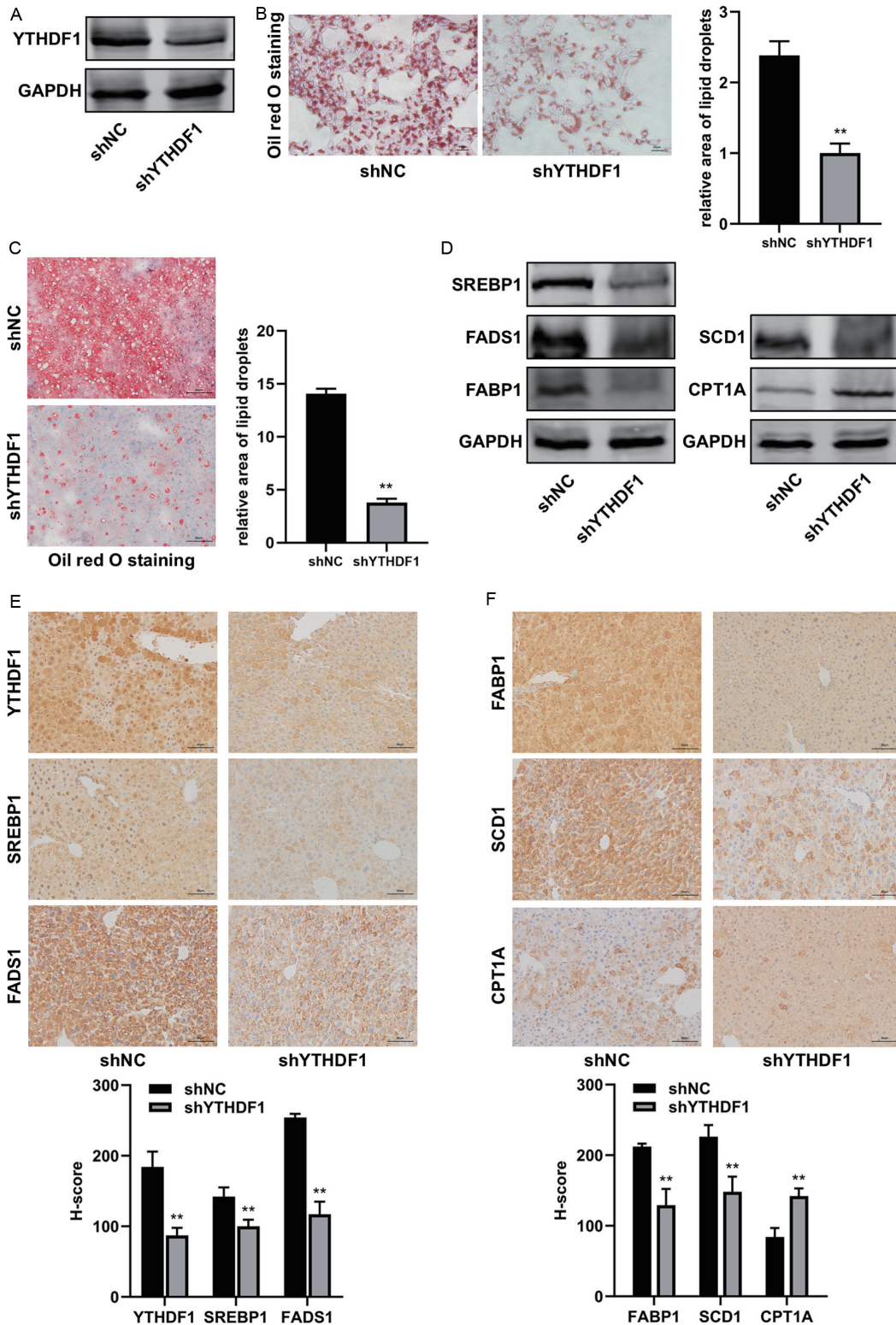


Fig. 3. Effect of YTHDF1 silencing on hepatic steatosis and lipid metabolism. (A) Western blot analysis of YTHDF1 expression in FFA-treated HepG2 cells transfected with shNC or shYTHDF1. (B) Oil Red O staining and quantification of lipid droplets in FFA-treated shNC and shYTHDF1 HepG2 cells. (C) Oil Red O staining and quantification of liver sections from HFD-fed mice injected with shYTHDF1 or shNC adenovirus ($n = 5$). (D) Western blot analysis of SREBP1, FADS1, FABP1, SCD1 and CPT1A protein levels in FFA-treated shNC and shYTHDF1 HepG2 cells. (E–F) IHC staining of YTHDF1, SREBP1, FADS1, FABP1, SCD1 and CPT1A in liver tissues from HFD-fed mice injected with shYTHDF1 or shNC adenovirus ($n = 5$). Data are shown as means \pm S.D. **** $P < 0.01$.** FFA, free fatty acids; HFD, high-fat diet; IHC, immunohistochemical; GAPDH, glyceraldehyde-3-phosphate dehydrogenase.

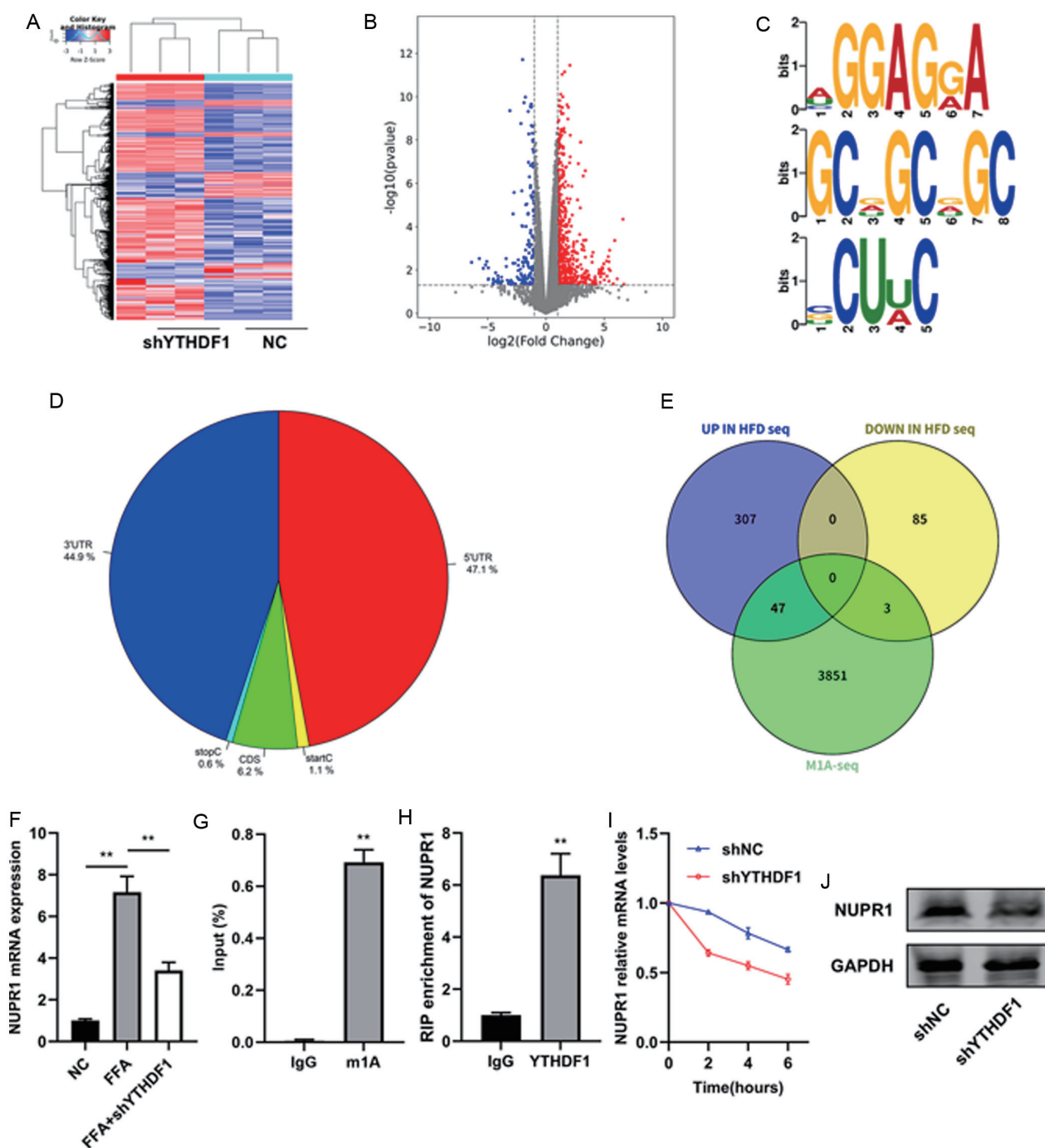


Fig. 4. Identification of NUPR1 as a key target of YTHDF1 in NAFLD. (A) Heatmap and (B) volcano plot of differentially expressed genes between shYTHDF1 and NC HepG2 cells. (C) Top three enriched motifs from m1A MeRIP-seq analysis in HepG2 cells. (D) Genomic distribution profile of m1A peaks across RNA regions (5' UTR, CDS, start codon, stop codon, 3' UTR) in HepG2 cells. (E) Venn diagram showing overlap among different expressed genes after FFA treatment and m1A MeRIP-seq (M1A-seq) data from HepG2 cells. (F) RT-qPCR analysis of NUPR1 mRNA expression in HepG2 cells under different conditions: NC, FFA treatment, and combined FFA treatment with YTHDF1 knockdown (FFA+shYTHDF1). (G) m1A-MeRIP-qPCR analysis of NUPR1 mRNA enrichment. IgG was used as a control. (H) RIP-qPCR analysis of the interaction between YTHDF1 protein and NUPR1 mRNA in HepG2 cells using an anti-YTHDF1 antibody. IgG was used as a negative control. (I) Assessment of NUPR1 mRNA stability by RT-qPCR in shNC and shYTHDF1 HepG2 cells following treatment with the transcriptional inhibitor actinomycin D (Act-D). (J) Western blot analysis of NUPR1 protein levels in shNC and shYTHDF1 HepG2 cells. Data are presented as mean \pm SD. *** $P < 0.01$. NAFLD, Non-alcoholic fatty liver disease; NC, negative control; FFA, free fatty acids.

in NAFLD. Emerging evidence has implicated RNA methylation as a critical post-transcriptional regulator of this process. In this study, we unveil a novel epitranscriptomic mechanism wherein the RNA methylation reader YTHDF1, which is

upregulated in NAFLD, promotes hepatic steatosis by specifically recognizing an m1A modification on NUPR1 mRNA, thereby stabilizing its transcript and enhancing lipogenesis.

The role of RNA methylation in NAFLD involves a complex

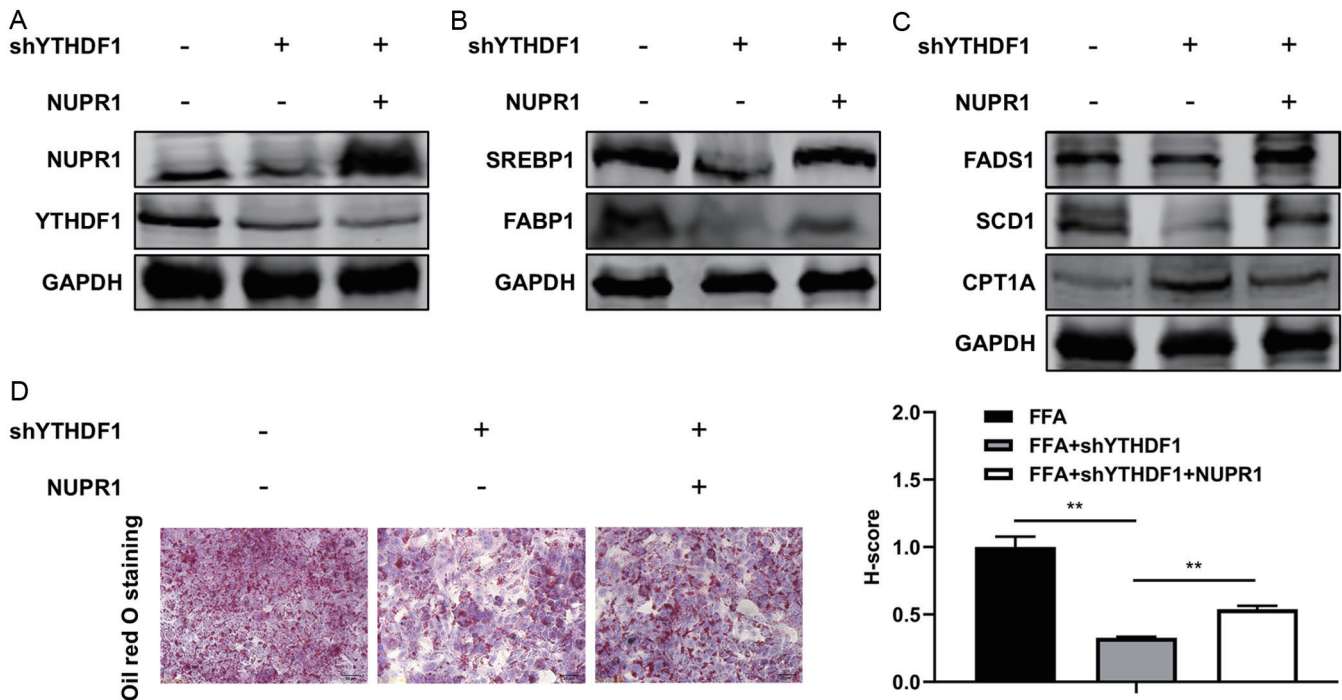


Fig. 5. Effect of NUPR1 overexpression on YTHDF1 knockdown-induced suppression of lipid accumulation. (A) Western blot analysis of NUPR1 and YTHDF1 expression in HepG2 cells subjected to different treatments: with (+) or without (-) YTHDF1 knockdown/NUPR1 overexpressing, all in the presence of free fatty acids (FFA). (B–C) Western blot analysis of lipogenesis (SREBP1, FABP1, FADS1, SCD1) and fatty acid oxidation-related proteins (CPT1A) in the same treatment groups. (D) Representative Oil Red O staining and quantitative analysis of lipid droplets in HepG2 cells from the three groups in under FFA treatment. Data are presented as mean \pm SD. $^{***}P < 0.01$. GAPDH, glyceraldehyde-3-phosphate dehydrogenase; FFA, free fatty acids.

network of writers, erasers, and readers. The m6A methyltransferase complex and reader YTHDF2 have been shown to promote steatosis,^{6,8,19} and the demethylase FTO can also facilitate lipid accumulation by enhancing lipid synthesis and suppressing lipolysis.²⁰ Similarly, the m1A demethylase ALKBH1 protects against diet-induced hepatic steatosis.²¹ We have identified a new driver within this complex regulatory network: YTHDF1, a protein found at elevated levels in NAFLD. YTHDF1 is a well-characterized reader of RNA modifications, best known for binding m6A to modulate mRNA stability and translation efficiency. However, its function is complex and may be context-dependent, with some studies even suggesting it could reduce mRNA stability under certain conditions.²² While YTHDF1 is known to contribute to NAFLD through its canonical function as an m6A reader, our findings reveal a previously unrecognized role: its pro-steatotic effect is also mediated through the recognition of m1A modifications. This discovery positions YTHDF1 as a dual-specificity reader that integrates two major epitranscriptomic signals, m6A and m1A, to exacerbate hepatic lipid dysregulation. The relevance of m1A recognition in this context is highlighted by the unique biochemical properties of this modification, which distinguish it from the more extensively studied m6A. Unlike m6A, which is predominantly enriched around the stop codon and within the 3'UTR, m1A carries a positive electrostatic charge under physiological conditions that disrupts Watson-Crick base pairing, potentially affecting RNA processing, structure, and protein interactions.^{23–30} Although m1A is a ubiquitous RNA modification with distribution patterns distinct from m6A, its specific readers and their functions in metabolic disease remain poorly defined. By demonstrating that YTHDF1 binds to the m1A-modified site within the NUPR1 3'UTR, this study provides the first evidence that YTHDF1's

m1A-reading capability has functional consequences in metabolic liver disease, expanding the current understanding of its regulatory capacity beyond its well-characterized m6A-mediated functions.

Mechanistically, we uncovered a YTHDF1–m1A–NUPR1 axis that drives hepatic steatosis. Under lipotoxic stress in hepatocytes, YTHDF1 binds to the m1A-modified site within the NUPR1 3'UTR. This interaction stabilizes NUPR1 mRNA, as evidenced by the reduced NUPR1 mRNA half-life upon YTHDF1 silencing. The functional relevance of this regulation was confirmed through rescue experiments: while YTHDF1 knockdown suppressed the expression of lipogenic genes (SREBP1, FADS1, FABP1, SCD1) and derepressed the fatty acid oxidation enzyme CPT1A, reintroducing NUPR1 in YTHDF1-deficient cells reversed these effects. These findings establish that YTHDF1 promotes lipogenesis and suppresses fatty acid oxidation through stabilizing NUPR1 mRNA. Together, these data establish m1A as a functionally relevant recognition substrate for YTHDF1 in the pathogenesis of hepatic steatosis, a role previously attributed only to m6A.

Collectively, this study demonstrates that YTHDF1 deficiency ameliorates hepatic steatosis by destabilizing NUPR1 mRNA through the loss of m1A recognition, leading to reduced lipogenesis. Nevertheless, several limitations of this work should be acknowledged. While YTHDF1 has been reported to promote steatosis through m6A recognition, our findings reveal an additional mechanism involving m1A-dependent NUPR1 stabilization. However, the relative contribution of these two recognition events to the overall pro-steatotic phenotype remains to be determined. Definitive proof of direct regulation would require mutation of the specific m1A site to disrupt YTHDF1 binding. Such experiments are technically challenging owing to the lack of a conserved consensus

sequence for m1A in mRNA, the limited resolution of current m1A mapping techniques, and the absence of well-established tools for site-specific manipulation of this modification. These constraints precluded definitive loss-of-function validation through point mutagenesis in this study. Additionally, the upstream regulators responsible for YTHDF1 upregulation in NAFLD remain unexplored and represent an important direction for future research.

These findings carry significant clinical implications despite the limitations discussed above. The YTHDF1–m1A–NUPR1 axis represents a highly specific and therapeutically actionable target. Unlike broad-spectrum approaches that globally disrupt RNA methylation machinery, which could lead to unintended off-target effects due to the essential cellular functions of these modifications, targeting the specific interaction between YTHDF1 and m1A-modified NUPR1 offers a more precise strategy to correct dysregulated lipogenesis. The dual specificity of YTHDF1 further suggests that blocking its RNA-binding domain could simultaneously disrupt both its m6A- and m1A-mediated pro-steatotic functions, potentially providing synergistic benefits. Beyond direct YTHDF1 targeting, the established role of NUPR1 as a stress-induced transcriptional regulator presents an additional therapeutic opportunity. Small molecules or antisense oligonucleotides targeting NUPR1 could be developed as complementary strategies for patients with YTHDF1-driven NAFLD. The elevation of YTHDF1 expression observed in both preclinical models and human NAFLD samples also raises its potential as a diagnostic or prognostic biomarker.

Conclusions

This study highlights the need for future preclinical efforts to develop and validate targeted therapies against this axis, paving the way for novel therapeutic strategies for the growing population of patients with NAFLD.

Funding

None to declare.

Conflict of interest

The authors have no conflict of interests related to this publication.

Author contributions

Performed cell and animal experiments involving Western blotting, qRT-PCR, IHC, H&E staining, and biochemical analysis (NL, ZX, DZ), conducted MeRIP assays (XY), conducted RIP assays (ZX), wrote the initial draft of the paper and were responsible for the preparation of figures (NL, YT), designed the experiments and critically reviewed the manuscript (YT, RL). All authors have approved the final version and publication of the manuscript.

Ethical statement

The study protocol received approval from the Laboratory Animal Center, Dalian Medical University (AEE23139) and conducted in accordance with the guide for the care and use of laboratory animals. All animals received human care.

Data sharing statement

Supporting data for this study are held by the correspond-

ing author and will be provided upon reasonable request for academic research purposes.

References

- [1] Meng L, Lu F, Zhang B, Ma Y, Gao J. Taming fatty liver: can taurine combat metabolic dysfunction in MASLD? *Cell Commun Signal* 2025;23(1):439. doi:10.1186/s12964-025-02439-x, PMID:41094516.
- [2] Yagüe-Caballero C, Casas-Deza D, Pascual-Oliver A, Espina-Cadena S, Arbones-Mainar JM, Bernal-Monterde V. MASLD-Related Hepatocarcinoma: Special Features and Challenges. *J Clin Med* 2024;13(16):4657. doi:10.3390/jcm13164657, PMID:39200802.
- [3] Liu J, Fu Q, Su R, Liu R, Wu S, Li K, *et al*. Association between nontraditional lipid parameters and the risk of type 2 diabetes and prediabetes in patients with nonalcoholic fatty liver disease: from the national health and nutrition examination survey 2017–2020. *Front Endocrinol (Lausanne)* 2024;15:1460280. doi:10.3389/fendo.2024.1460280, PMID:39280011.
- [4] Kang M, Song J, Kang ES, Jang S, Kwak T, Kim Y, *et al*. Pathophysiology, development, and mortality of major non-communicable diseases in metabolic dysfunction-associated steatotic liver disease: A comprehensive review. *Int J Biol Sci* 2025;21(13):5691–5703. doi:10.7150/ijbs.117211, PMID:41079926.
- [5] Fan JG, Xu XY, Yang RX, Nan YM, Wei L, Jia JD, *et al*. Guideline for the Prevention and Treatment of Metabolic Dysfunction-associated Fatty Liver Disease (Version 2024). *J Clin Transl Hepatol* 2024;12(11):955–974. doi:10.14218/JCTH.2024.00311, PMID:39544247.
- [6] Meng J, Yan C, Liu J. LDHA-Mediated Histone Lactylation Promotes the Nonalcoholic Fatty Liver Disease Progression Through Targeting the METTL3/YTHDF1/SCD1 m6A Axis. *Physiol Res* 2024;73(6):985–999. doi:10.33549/physiolres.935289, PMID:39903889.
- [7] Peng Z, Gong Y, Wang X, He W, Wu L, Zhang L, *et al*. METTL3-m(6)A-Rubicon axis inhibits autophagy in nonalcoholic fatty liver disease. *Mol Ther* 2022;30(2):932–946. doi:10.1016/j.ymthe.2021.09.016, PMID:34547464.
- [8] Wang YF, Zhang WL, Li ZX, Liu Y, Tan J, Yin HZ, *et al*. METTL14 downregulation drives S100A4(+) monocyte-derived macrophages via MyD88/NF-κB pathway to promote MAFLD progression. *Signal Transduct Target Ther* 2024;9(1):91. doi:10.1038/s41392-024-01797-1, PMID:38627387.
- [9] He Y, Wang W, Xu X, Yang B, Yu X, Wu Y, *et al*. Mettl3 inhibits the apoptosis and autophagy of chondrocytes in inflammation through mediating Bcl2 stability via Ythdf1-mediated m(6)A modification. *Bone* 2022;154:116182. doi:10.1016/j.bone.2021.116182, PMID:34530171.
- [10] Wang L, Zhu L, Liang C, Huang X, Liu Z, Huo J, *et al*. Targeting N6-methyladenosine reader YTHDF1 with siRNA boosts antitumor immunity in NASH-HCC by inhibiting EZH2-IL-6 axis. *J Hepatol* 2023;79(5):1185–1200. doi:10.1016/j.jhep.2023.06.021, PMID:37459919.
- [11] Long JK, Dai W, Zheng YW, Zhao SP. miR-122 promotes hepatic lipogenesis via inhibiting the LKB1/AMPK pathway by targeting Sirt1 in non-alcoholic fatty liver disease. *Mol Med* 2019;25(1):26. doi:10.1186/s10020-019-0085-2, PMID:31195981.
- [12] Felgner PL, Gadek TR, Holm M, Roman R, Chan HW, Wenz M, *et al*. Lipofection: a highly efficient, lipid-mediated DNA-transfection procedure. *Proc Natl Acad Sci U S A* 1987;84(21):7413–7417. doi:10.1073/pnas.84.21.7413, PMID:2823261.
- [13] Mahmood T, Yang PC. Western blot: technique, theory, and trouble shooting. *N Am J Med Sci* 2012;4(9):429–434. doi:10.4103/1947-2714.100998, PMID:23050259.
- [14] Livak KJ, Schmittgen TD. Analysis of relative gene expression data using real-time quantitative PCR and the 2(-Delta Delta C(T)) Method. *Methods* 2001;25(4):402–408. doi:10.1006/meth.2001.1262, PMID:11846609.
- [15] Ahmed I, Mohamed A, Savari O, Xue Y, Asa SL. Expression of DLL3 and SEZ6 in the Spectrum of Neuroendocrine Neoplasia. *Endocr Pathol* 2025;36(1):27. doi:10.1007/s12022-025-09873-0, PMID:40699376.
- [16] Peritz T, Zeng F, Kannanayakal TJ, Kilk K, Eiríksdóttir E, Langel U, *et al*. Immunoprecipitation of mRNA-protein complexes. *Nat Protoc* 2006;1(2):577–580. doi:10.1038/nprot.2006.82, PMID:17406284.
- [17] Li X, Xiong X, Zhang M, Wang K, Chen Y, Zhou J, *et al*. Base-Resolution Mapping Reveals Distinct m(1)A Methylome in Nuclear- and Mitochondrial-Encoded Transcripts. *Mol Cell* 2017;68(5):993–1005.e9. doi:10.1016/j.molcel.2017.10.019, PMID:29107537.
- [18] Zheng Q, Gan H, Yang F, Yao Y, Hao F, Hong L, *et al*. Cytoplasmic m(1)A reader YTHDF3 inhibits trophoblast invasion by downregulation of m(1)A-methylated IGF1R. *Cell Discov* 2020;6:12. doi:10.1038/s41421-020-0144-4, PMID:32194978.
- [19] Wang Y, Tian X, Wang Z, Liu D, Zhao X, Sun X, *et al*. A novel peptide encoded by circ-SLC9A6 promotes lipid dyshomeostasis through the regulation of H4K16ac-mediated CD36 transcription in NAFLD. *Clin Transl Med* 2024;14(8):e1801. doi:10.1002/ctm2.1801, PMID:39107881.
- [20] Pan J, Ye W, Zhang J, Fan Y, Chen Z, Wang Y, *et al*. Knockdown of Salusin-β Downregulates FTO to Inhibit Lipid Synthesis and Promote Lipolysis to Attenuate NAFLD. *Liver Int* 2025;45(9):e70252. doi:10.1111/liv.70252, PMID:40729528.
- [21] Luo L, Liu Y, Nizigiyimana P, Ye M, Xiao Y, Guo Q, *et al*. DNA 6mA Demethylase ALKBH1 Orchestrates Fatty Acid Metabolism and Suppresses Diet-Induced Hepatic Steatosis. *Cell Mol Gastroenterol Hepatol* 2022;14(6):1213–1233. doi:10.1016/j.jcmgh.2022.08.011, PMID:36058506.
- [22] Lei Y, Zhan E, Chen C, Hu Y, Lv Z, He Q, *et al*. ALKBH5-mediated m(6)A demethylation of Runx2 mRNA promotes extracellular matrix degradation and intervertebral disc degeneration. *Cell Biosci* 2024;14(1):79.

- doi:10.1186/s13578-024-01264-y, PMID:38877576.
- [23] Agris PF. The importance of being modified: roles of modified nucleosides and Mg²⁺ in RNA structure and function. *Prog Nucleic Acid Res Mol Biol* 1996;53:79–129. doi:10.1016/s0079-6603(08)60143-9, PMID:8650309.
- [24] Woo HH, Chambers SK. Human ALKBH3-induced m(1)A demethylation increases the CSF-1 mRNA stability in breast and ovarian cancer cells. *Biochim Biophys Acta Gene Regul Mech* 2019;1862(1):35–46. doi:10.1016/j.bbagr.2018.10.008, PMID:30342176.
- [25] Wu Y, Chen Z, Xie G, Zhang H, Wang Z, Zhou J, *et al*. RNA m(1)A methylation regulates glycolysis of cancer cells through modulating ATP5D. *Proc Natl Acad Sci U S A* 2022;119(28):e2119038119. doi:10.1073/pnas.2119038119, PMID:35867754.
- [26] Li X, Xiong X, Wang K, Wang L, Shu X, Ma S, *et al*. Transcriptome-wide mapping reveals reversible and dynamic N(1)-methyladenosine methylome. *Nat Chem Biol* 2016;12(5):311–316. doi:10.1038/nchembio.2040, PMID:26863410.
- [27] Dominissini D, Nachtergaele S, Moshitch-Moshkovitz S, Peer E, Kol N, Ben-Haim MS, *et al*. The dynamic N(1)-methyladenosine methylome in eukaryotic messenger RNA. *Nature* 2016;530(7591):441–446. doi:10.1038/nature16998, PMID:26863196.
- [28] Safra M, Sas-Chen A, Nir R, Winkler R, Nachshon A, Bar-Yaacov D, *et al*. The m1A landscape on cytosolic and mitochondrial mRNA at single-base resolution. *Nature* 2017;551(7679):251–255. doi:10.1038/nature24456, PMID:29072297.
- [29] Zhang LS, Xiong QP, Peña Perez S, Liu C, Wei J, Le C, *et al*. ALKBH7-mediated demethylation regulates mitochondrial polycistronic RNA processing. *Nat Cell Biol* 2021;23(7):684–691. doi:10.1038/s41556-021-00709-7, PMID:34253897.
- [30] Zhou H, Kimsey IJ, Nikolova EN, Sathyamoorthy B, Grazioli G, McSally J, *et al*. m(1)A and m(1)G disrupt A-RNA structure through the intrinsic instability of Hoogsteen base pairs. *Nat Struct Mol Biol* 2016;23(9):803–810. doi:10.1038/nsmb.3270, PMID:27478929.